



LAWRENCE
LIVERMORE
NATIONAL
LABORATORY

Advanced NDE Techniques for Powder Metal Components

P. Martin, J. Haskins, G. Thomas, K. Dolan

May 1, 2003

2003 International Conference on Powder Metallurgy and
Particulate Materials,
Las Vegas, Nevada, June 8-12-2003

This document was prepared as an account of work sponsored by an agency of the United States Government. Neither the United States Government nor the University of California nor any of their employees, makes any warranty, express or implied, or assumes any legal liability or responsibility for the accuracy, completeness, or usefulness of any information, apparatus, product, or process disclosed, or represents that its use would not infringe privately owned rights. Reference herein to any specific commercial product, process, or service by trade name, trademark, manufacturer, or otherwise, does not necessarily constitute or imply its endorsement, recommendation, or favoring by the United States Government or the University of California. The views and opinions of authors expressed herein do not necessarily state or reflect those of the United States Government or the University of California, and shall not be used for advertising or product endorsement purposes.

ADVANCED NDE TECHNIQUES FOR POWDER METAL COMPONENTS

Peter Martin, Jerry Haskins, Graham Thomas, and Ken Dolan

**Nondestructive Evaluation
Lawrence Livermore National Laboratory
Livermore, CA 94550**

ABSTRACT

Nondestructive evaluation encompasses numerous technologies that assess materials and determine important properties. This paper demonstrates the applicability of several of these technologies to the field of powder metallurgy. The usual application of nondestructive evaluation is to detect and quantify defects in fully sintered product. But probably its most appealing role is to sense problems earlier in the manufacturing process to avoid making defects at all. Also nondestructive evaluation can be incorporated into the manufacturing processes to monitor important parameters and control the processes to produce defect free product. Nondestructive evaluation can characterize powders, evaluate components in the green state, monitor the sintering process, and inspect the final component.

INTRODUCTION

Powder metallurgy (PM) refers to the class of techniques used to produce metallic components by the solid state densification of a precursor powder. PM techniques are used for processing a wide variety of components ranging from light bulb filaments to complex shaped automotive parts. In these techniques, the precursor powder is compacted (pressed) into a near net-shape preform called the 'green' state. The high surface area and curvature associated with the powder particles provide a strong thermodynamic driving force for densification when the green compact is heated to temperatures significantly below the melting point. Since the PM component can be produced at a temperature below the melting point,

significant cost (energy) savings can be realized. Additional savings result from the reduction in machining costs associated with the near net-shape capability of the PM process, particularly for complex parts. Additionally, low processing temperatures allow the use of pre-alloyed powders, and reduce the risk of phase segregation during processing. The net result is that PM processing can provide reduced cost components with enhanced, and possibly unique, properties relative to traditional processing methods.

The automotive industry is currently integrating an increasing number of PM components into their production capabilities. For the potential benefits of this technology to be fully realized, however, the capability must be developed to apply PM processing to the mass production of complex shaped components with a minimal reject rate. Initial testing of PM components has identified several broad areas of research which are critical to the development of this capability. These can be essentially distilled to two fundamental issues: i) reliability testing of green components, and ii) enhanced understanding of the interrelationship between process parameters and defect formation. The former relates to the mitigation of losses associated with defective parts by allowing rejection prior to the expense of firing and machining. Also, unlike fired components, the raw materials from rejected green components can often be recycled. The latter issue pertains to optimizing the process parameters to prevent the formation of process-induced defects.

Powder metallurgy has enjoyed an enviable position among metal working technologies, and improved its position against other near net shape technologies, such as casting and forging. Improvement in dynamic properties of powder metallurgy materials has led the growth of powder metallurgy in the late 80's and early 90's. The main benefactors of these property improvements have been engine components; namely connecting rod and crankshaft bearing retainer caps. In fact, powder metallurgy is the preferred, cost effective choice for stainless steel exhaust system flanges and near-manifold bosses. Exhaust system applications have led the current wave of powder metallurgy growth, which is being driven by governmental emissions standards calling for 50,000 mile, no-exhaust gas leakage. New automotive powertrain applications of the last decade have insured continued powder metal growth into the 21st century. If further improvements in dimensional capability of the powder metallurgy process can be gained, then nodular iron transmission gearing offers potential for the next generation of conversions. Most of the potential applications require not only high load carrying capacity, but also a high degree of dimensional accuracy. The combination of these two qualities is termed Power Density.

Many factors are driving the automobile industry towards use of higher power density components. Custom demands for increased performance translates into the transmission gearing handling higher

engine output torques. Also, mandates to improve fuel economy with reduced emission levels leads future vehicle designs toward weight and size reductions. This reduces the real estate available for the powertrain, as well as the size and weight of individual components. With increasing loads from the engine, dimensional accuracy of power transfer gearing becomes more important as a means of keeping the stress levels within design limits.

APPLICATIONS

Three different areas of study are currently being considered - Computed tomography (CT) of metal powder, CT of pressed powder specimens, and ultrasonic testing (UT) of pressed, sintered powder specimens.

CT of Powder Metal

The flow and fill properties of powders into the shoe and die cavity were investigated to evaluate the usefulness of computed tomography (CT) for powder metal diagnostics. These powder characteristics are believed to be a major contributor to dimensional inconsistency in powder metallurgy parts. The resulting spatial distributions in the powder packing (density) were evaluated using CT and are reported here.

CT data is particularly suited for powder metal studies because the discrete data packets which result from the data reconstruction quantitatively represent discrete volume elements. The data in the previous study consisted of approximately 252 million volume elements. Each volume element was 125 μ on a side. This was reduced to 700 vertical slice planes, which were being converted to slice planes in two other dimensions. The advantage of CT in this case was the opportunity to analyze micro-volumes at greater sensitivity than possible with radiography and more cost effectively as compared to metalography. Two powder mixes were used in this study, one a standard base material blend and one treated with a binder to enhance flow. These powder grades were selected because of their potential use as gearing materials. Gearing alloys must have sufficient harden ability to respond to induction heating. Widely differing flow characteristics were sought, to see if computed tomography can detect fill density differences. The data for this experiment was acquired with a medium energy lens-coupled scanner with the following experimental parameters:

Photometrics cooled 14 bit camera, 1024 x 1024 pixels

6 mm thick IQI LKH-6 scintillator glass

0.080" Cu filter

PHILIPS 450 kVp x-ray source

5" field of view

125 μ pixels

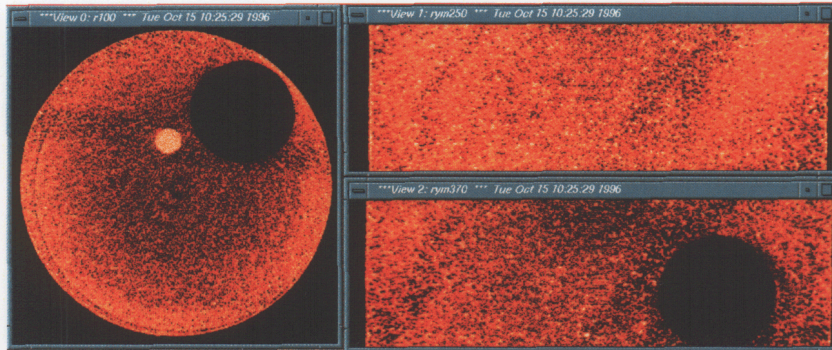


Figure 1: Packing Uniformity.

Initial tests were performed using a 3" diameter cup to determine whether adequate sensitivity is available for these tests. Figure 1 demonstrates the effect on packing uniformity around spherical objects. Figure 2 is a histogram of particle size distribution. This technique could be used to detect and track particle segregation by size. Figure 3 is a vertical CT slice through the die with curves representing the relative density along a vertical profile for both treated and untreated powder. There is less densification of the powder at the top of the die with the treated powder. Treated and untreated powders generally behave similarly except at top of die where the treated powder shows less densification.

Figure 4 is a vertical CT slice through the die accompanied by two horizontal slices at the positions shown. Data profiles across these horizontal slices show an apparently higher density near the outer (concave) surfaces of the die and lower density near the inner (convex) surfaces.

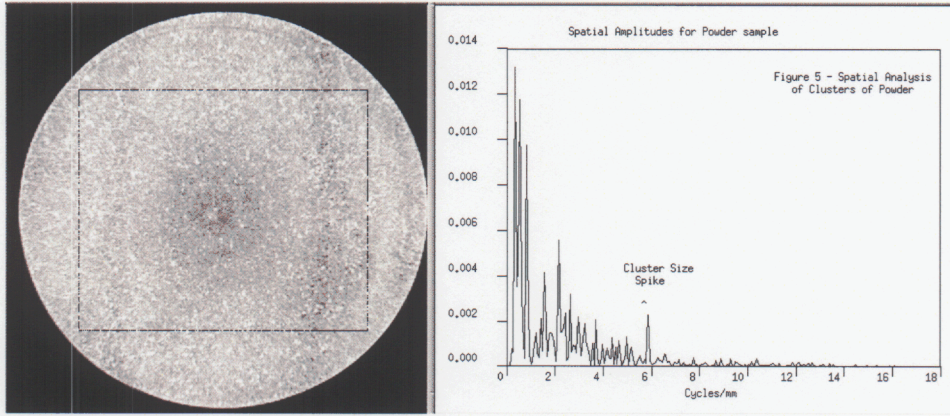


Figure 2: Particle Size Analysis.

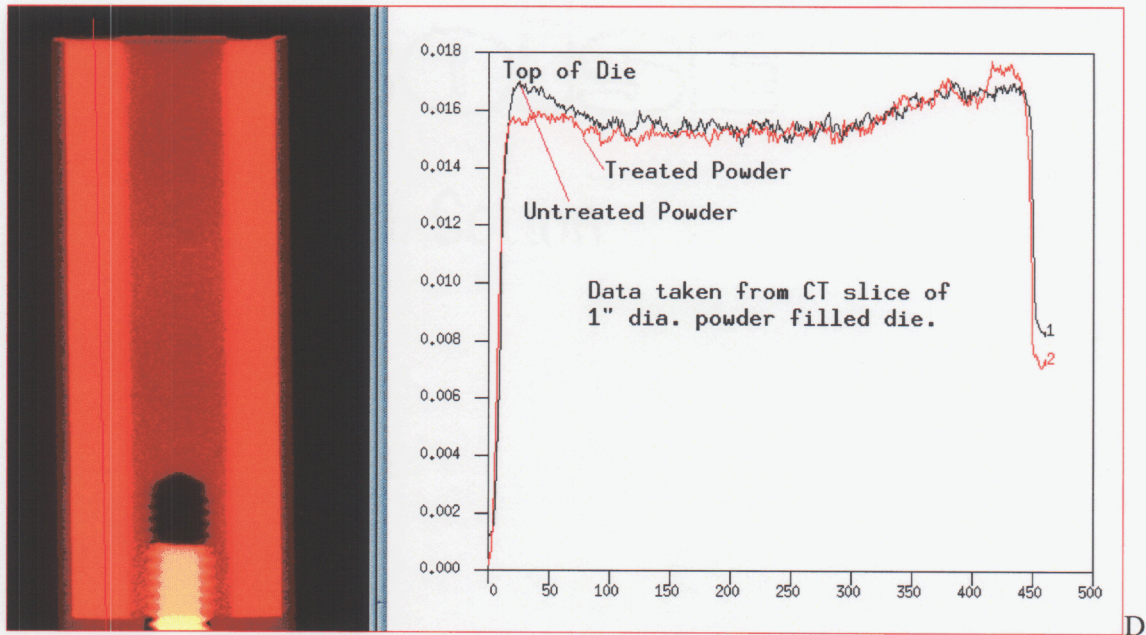


Figure 3: Vertical Data Slice of Powder Density.

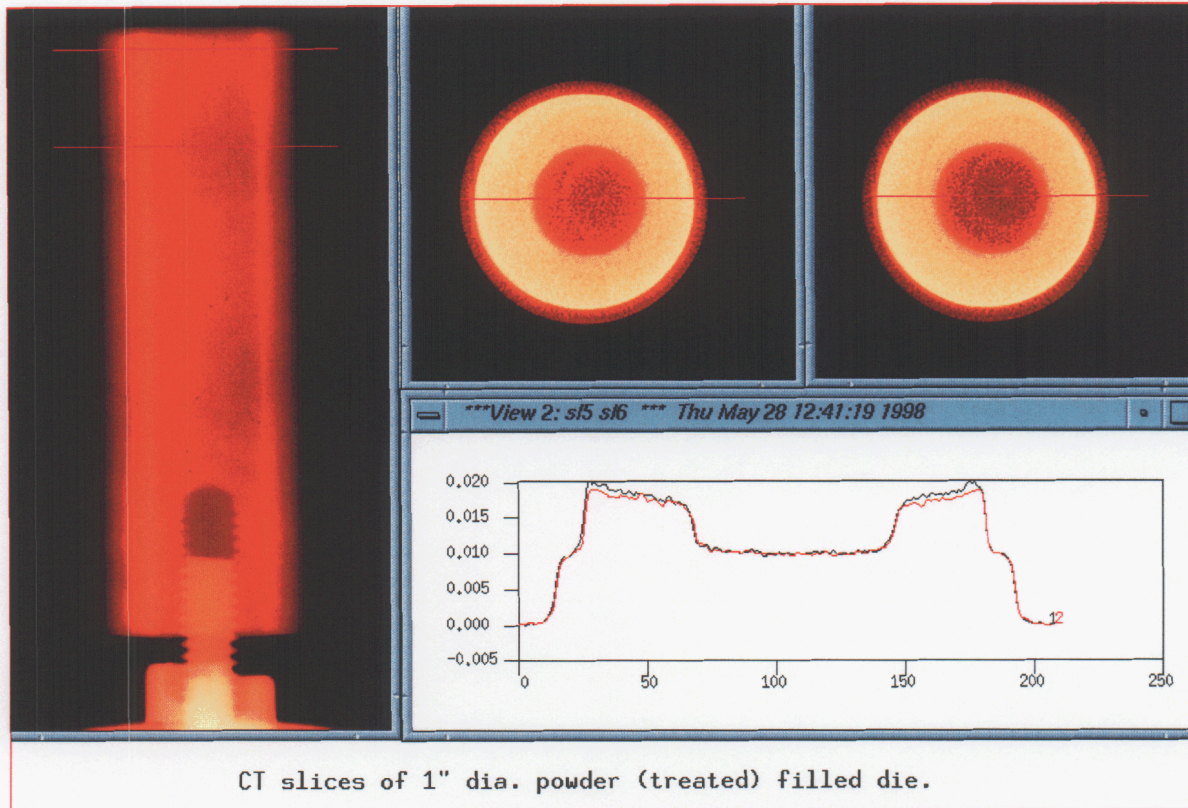


Figure 4: Horizontal Data Slices.

Conclusions from Powder Study

A difference in the flow characteristics between the two powders was indeed be detected. The powders exhibited a 15% difference in flow. This is especially apparent in Figure 3 which compares vertical density plots for treated and untreated powder. The enhanced flow characteristics of the treated powder suggest lower intergranular friction. The shoe motion exerts an angled downward force due to static head pressure of extra powder in shoe and the horizontal velocity vector as the shoe is translated across powder mass. The resultant down force appears to be better transferred through the packed bed in the lower friction powder.

In Figure 4 the powder density appears to be higher near the concave die surfaces than near the convex die surfaces. If this is real, then filling die/core rod(s) sets with slots, teeth and other geometric discontinuities should alter the density uniformity. This means that tooth die and core rod cavities oriented along the axis of the shoe motion should pack greater than those that are off axis should. This suggests that a different way of filling should be explored. Ideally the fill should be in the same axis as the tool motion and sharp corners should be avoided.

Absolute density differences can be determined with these techniques. The accuracy of this measurement has yet to be determined for powders but doing so presents no technical problems. We expect that absolute density could be determined to within 1% to 2% and that determination of relative density differences may be much more precise. Meaningful data may actually require larger (lower resolution) sampling volumes to avoid statistical variations.

Pressed Powder Studies

Technically the goal is to demonstrate our diagnostic capabilities on pressed and sintered parts. General Motors supplied ring gears and connecting rods. Initial work has involved the ring gears. CT scans on sections of a ring gear showed the features around the gear teeth and at the root region that had been destructively detected with sectioning and metallography in other samples. Figure 5 shows a y-slice and a z-slice with a prominent defect region.

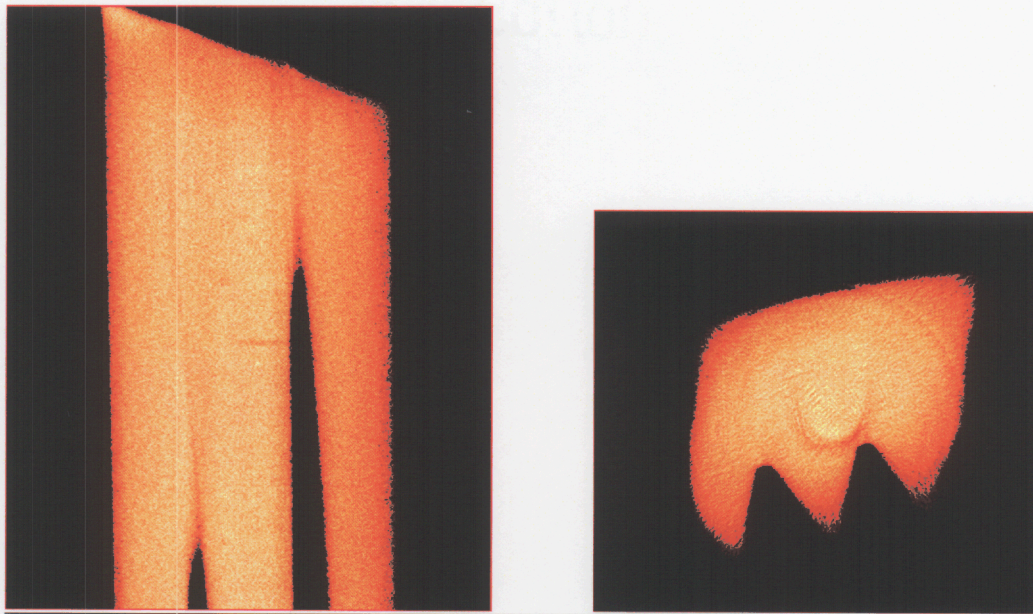


Figure 5: Y and Z slices through ring gear sample.

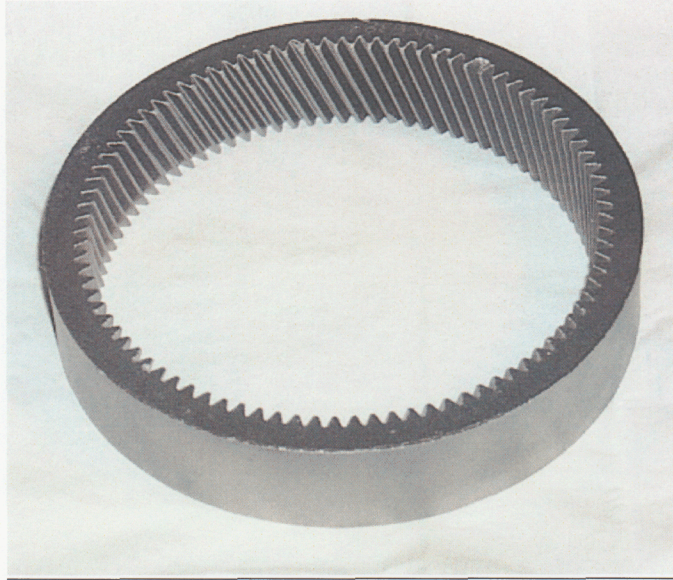


Figure 6: Photograph of Ring Gear.

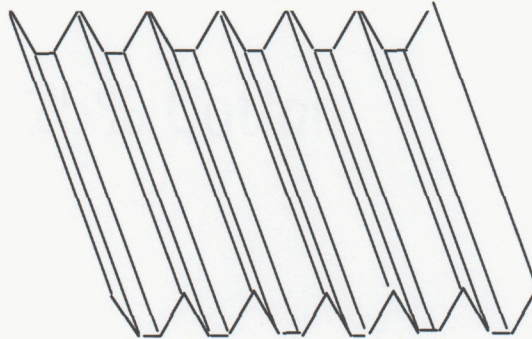


Figure 7: Sketch of Ring Gear Tooth Profile.

The ring gears evaluated are approximately 5 3/4" OD by 4 3/4" ID and 1 1/8" high. Each gear has 90 teeth on the ID running at approximately 20° as shown in Figures 6 & 7. The features of concern lie at the root of the teeth and in layers along the sides of the teeth as shown in Figure 8. These layers can be detected using metallography but success depends on chance and the number of sections polished. Much of the current focus is on improving the sensitivity of the CT scan and on better ways to evaluate the large data sets obtained. The initial data obtained showed anomalies close to the gear teeth as expected. Later data showed anomalies at other locations and in other orientations. Figure 8 below shows a radiograph with vertical and horizontal CT slices through regions with anomalies.

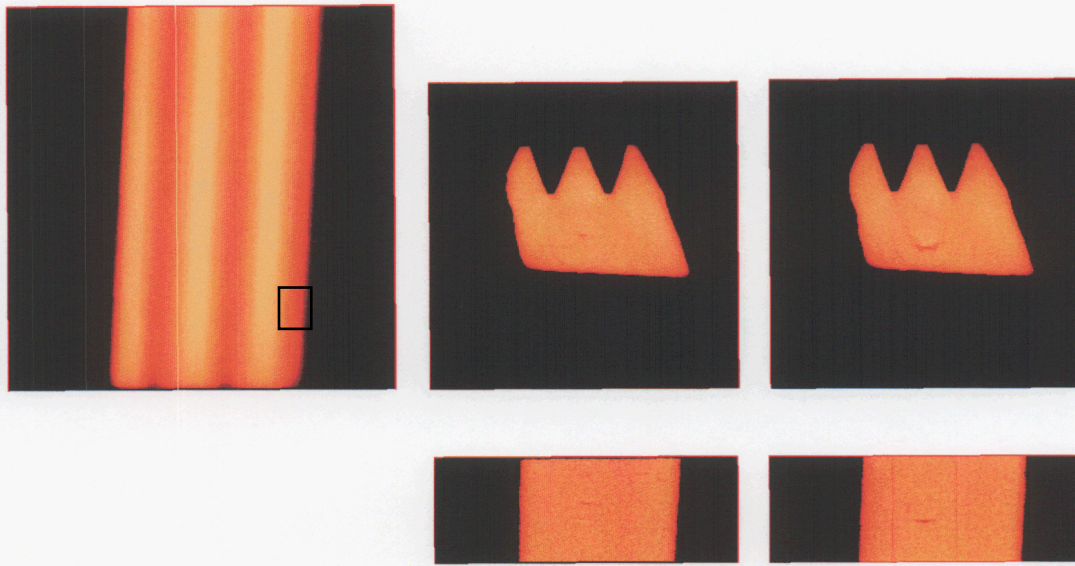


Figure 8: Radiograph and CT Slices of Section of Ring Gear.

Ultrasonic Testing (UT) Of Pressed, Sintered Powder Specimens

In ultrasonic testing, the component is insonified with a beam of sound waves with a frequency above the range of human hearing. Often, the component is immersed in water to facilitate coupling of the sound waves into the material. Alternate liquids may be used to accommodate corrosive and/or acoustic requirements. For testing of the automotive transmission ring gears, the gears were immersed in water and insonified with a focussed, 30 MHz frequency transducer. The transducer was positioned with a multiple axis scanning system to provide areal coverage of the part. Sound waves enter through the outside (circumferential) face of the gear and are reflected back to the transducer by any discontinuities in the material including cracks, voids, and the boundary of the component. The raw data consist of amplitude (voltage) versus time of flight of the sound waves from the transducer to the reflecting discontinuity and back to the transducer. From the sound wave velocity in the material, this time can be used to determine the defect depth. It is common practice to correlate the signal amplitude with a calibrated defect of known size, such as a flat-bottomed hole. The data can be presented in several different ways. An A-scan is the raw amplitude versus time-of flight data described above, and this is what is seen on an oscilloscope screen. This provides most of the important information regarding the acoustic signal, but is not easily interpreted by the untrained operator. An example of an A-scan is shown in Figure 9, where the amplitude of the acoustic signal is plotted as a function of time-of-flight. The

moderate amplitude signal at 30.50 μs an artifact of the experimental method and does not represent an internal discontinuity. The large signal at 31.75 ms is the bottom of a notch between two gear teeth.

The measurements were configured in such a fashion that the sound waves were focussed to the base of the gear teeth (the bottom of the notches). This was done because the principal defects of interest are discontinuities related to low powder packing density in that vicinity. While the A-scan shown above contains all the pertinent information for testing one location on the gear, it is often of interest to scan over large areas and present the data as a false-color image. To accomplish this the data are gated to select only arrival times corresponding to the region of interest, in this case the region encompassing ~ 6 mm below the base of the gear teeth. The maximum value of the signal in the gate is plotted as a function of position. This presentation of the data is called a C-scan, a sample of which is shown in Figure 10. The data are useful for locating discontinuities which may be buried in a large volume; however care must be taken in interpretation due to the color-amplitude correlation. The signal amplitude can be significantly affected by changes in surface quality and/or orientation. Given that the ring gears in question were significantly out-of-round, and also had some surface curvature in the axial direction it is difficult to correlate amplitude measured at different locations without optimizing the alignment at each location.

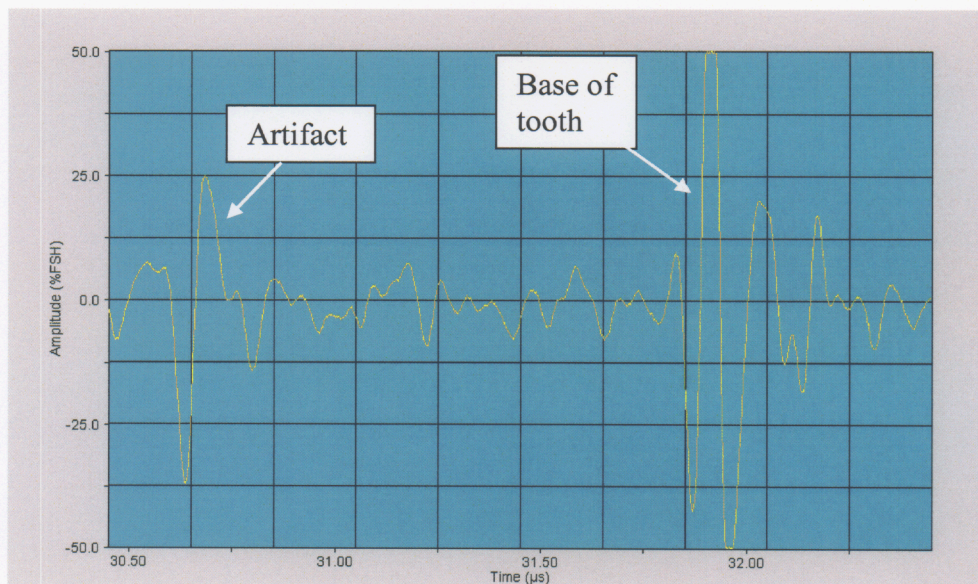


Figure 9: An ultrasonic A-scan showing signal amplitude versus travel time for sound waves reflected from the base of the notch between two gear teeth.

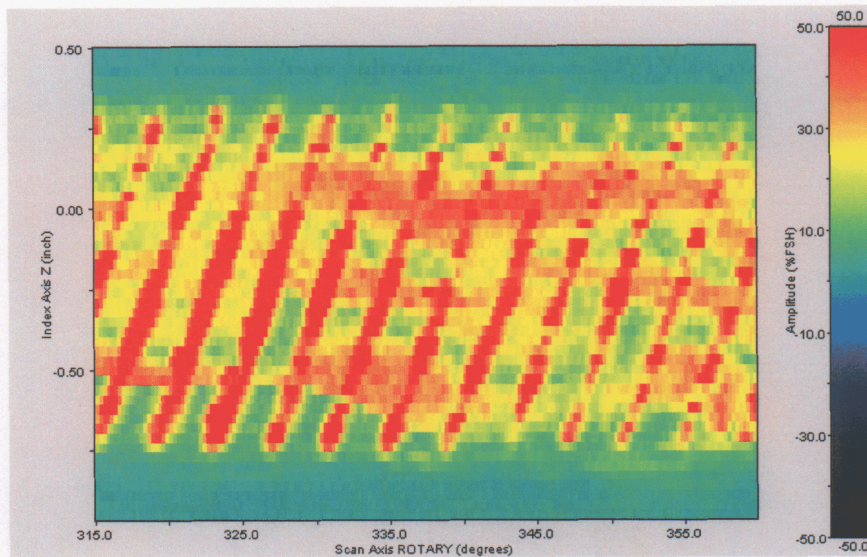


Figure 10: C-scan image of a 45° section of a ring gear. Color is proportional to signal amplitude. The gate is set to interrogate 6 mm below the base of the gear teeth.

Another useful technique for projecting the A-scan acoustic data into an image is to plot travel time as a function of position along one axis (i.e. rotation in degrees) while the coordinate in the other axis (i.e. axial-translation) is held constant. This type of cross-sectional image is called a B-scan, and provides an excellent diagnostic capability for the ring gear inspection. This presentation of the data is comparable to a radiographic CT slice. The primary benefit from the B-scan presentation is that the viewer is presented with not only amplitude information, which is again correlated to color, but to arrival time information. As can be seen in Figure 11, where a B-scan corresponding to a slice across the $z = -0.25''$ section from Figure 10, the presence of a discontinuity reflection is immediately apparent.

The observed discontinuity return in Figure 11 is a clear indication of a significant discontinuity in the part. The location of the discontinuity is slightly over 1 mm below the base of the teeth. The gear tooth geometry is indicated schematically at the right side of the figure. It should be noted that these types of discontinuities were observed at various depths in the component, even near the surface. However, for the purpose of the current study, the defects of primary interest are in the region around the base of the teeth since this is the most problematic location in terms of potential gear (tooth) failure.

Note the 'wavy' front running across the image in Figure 11 at approximately 30.50 - 30.75 μs . This front corresponds to the artifact noted in Figure 9. This artifact corresponds to a spurious (multiple path) echo from the front face of the specimen. Thus, while the location of the echo does not correlate to any

physical feature of the component at the corresponding depth in the material, the shape (i.e. 'waviness') corresponds to the degree to roundness of the outside circumference of the part. The waviness in the Figure corresponds to approximately 0.5 mm of surface displacement. Note that the gear tooth echoes follow the surface displacement, so the indication is not of varying thickness but rather of constant thickness and an out-of-round condition. An A-scan corresponding to the line indicated in Figure 11 is shown in Figure 12. Note the large signal at 31.5 μ s, corresponding to the discontinuity, compared with the absence of this signal in the discontinuity-free A-scan shown in Figure 9.

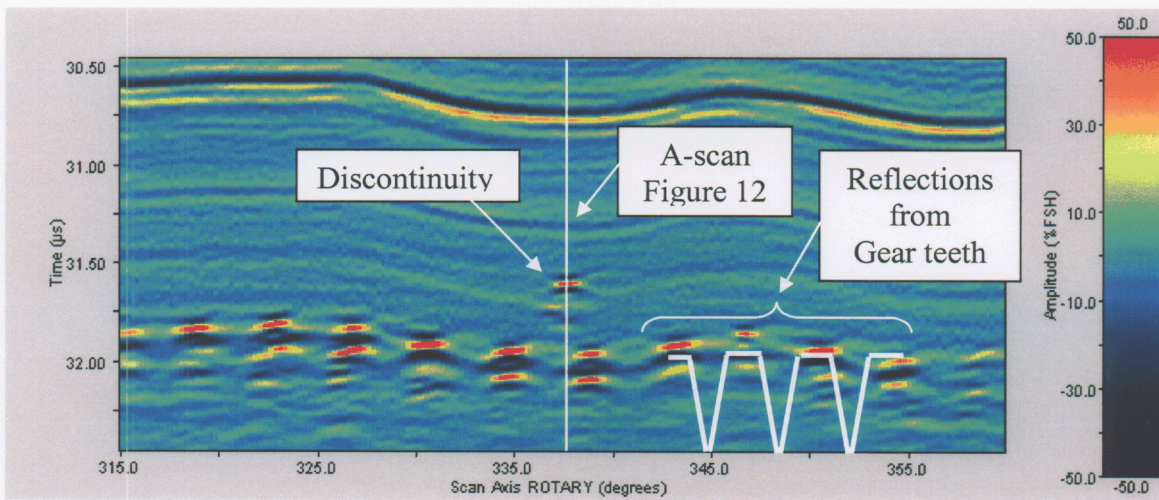


Figure 11: B-scan showing time of flight of the acoustic signal versus degrees around the ring gear (from 315-360°). Color is proportional to signal amplitude. Note the discontinuity return at ~338°. The gear teeth are indicated schematically, and the vertical white line indicates the location of the A-scan shown in Figure 12.

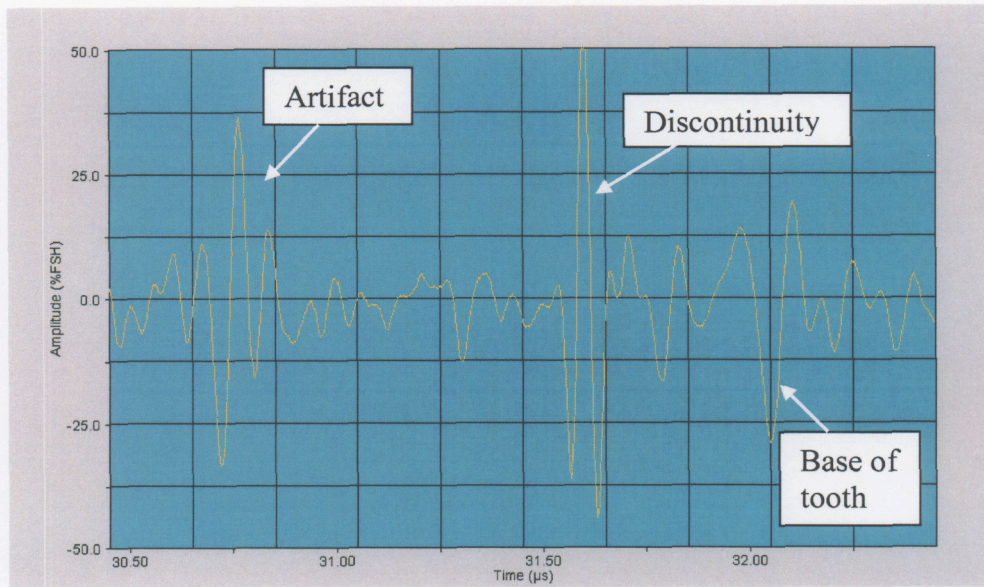


Figure 12: A-scan showing amplitude versus time of flight of the acoustic signal corresponding to the white line in Figure 11.

Once the defect location has been determined via the B-scan coordinates, it is possible to move the transducer to that location, optimize the alignment to the surface orientation at that location, and perform a high resolution C-scan to, in effect, view the discontinuity. This was performed for the discontinuity noted in Figure 11, and is shown in Figure 13. From that analysis, it can be seen that the *approximate* dimensions of the discontinuity are 0.05” in the z-axis and 1.5° around the circumference. Given the location of the discontinuity, this corresponds to a circumferential dimension of approximately 0.07”. It should be noted that this calculation should, to be precise, account for other factors such as beam diffraction and spot size. As mentioned earlier, the standard technique for quantifying the discontinuity characteristics is to compare the acoustic data to a known reflector with comparable echo amplitude, usually a flat bottomed hole.

Conclusions from UT Study

The following conclusions can be drawn from the data acquired during the ultrasonic testing of the ring gears:

- There are discontinuities present in the component.
- These discontinuities can be located and sized using ultrasonic testing.
- The discontinuities do not appear to occur at any characteristic depth or location.

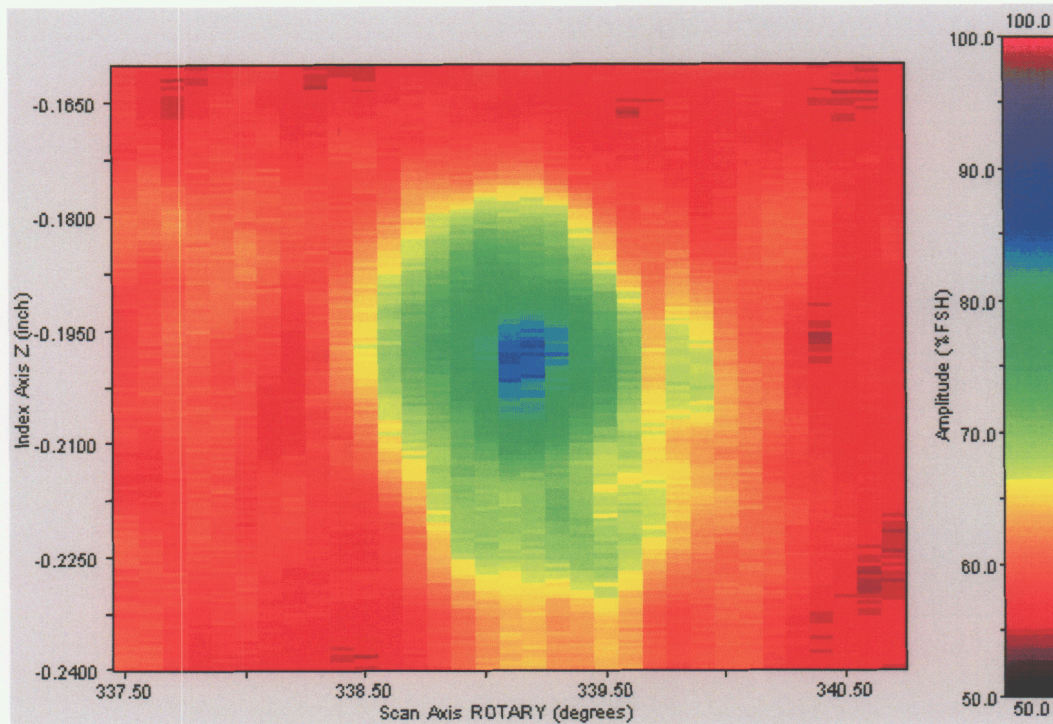


Figure 13: Ultrasonic C-scan around the region noted as a discontinuity signal in Figure 11.

SUMMARY

The work described in this paper clearly demonstrates the benefit of incorporating nondestructive evaluation technologies into the field of powder metallurgy. The paper does not address all possible techniques or all possible applications. For example, depending on the type of defect to be detected or the process to be monitored one might incorporate eddy current, thermal, acoustic emission, or optical techniques. A close collaboration between nondestructive evaluation experts and powder metal scientists is needed to fully exploit the potential.

This work was performed under the auspices of the U.S. Department of Energy by the University of California, Lawrence Livermore National Laboratory under Contract No. W-7405-Eng-48.